Development and Testing of a Novel Low-Cost LEO Optical Surveillance Sensor

Borja Del Campo López, Emma Kerr
DEIMOS Space UK Ltd, Airspeed 1, 151 Eighth Street, Harwell Campus, OX11 0RL, UK
emma.kerr@deimos-space.com
Jaime Nomen Torres
DEIMOS Engineering and Systems, Calle Francia 9, 13500 Puertollano, Spain
Chris Dorn
Inverse Quanta Ltd, Brooklands, Pankridge Street, Crondall, Hampshire, GU10 5QU, UK
Stuart Eves
SJE Space Ltd., 29 Clayhill Road, Burghfield Common, Berkshire, RG7 3HB UK

ABSTRACT

Optical tracking of LEO objects has been extensively studied and exercised. A novel surveillance method using an array of collocated fixed Field of View telescopes and the development of a dedicated image processing software is described. The Low-Cost Low-Earth Orbit Surveillance Sensor Array (LCLEOSEN) has been developed to target a similar market as conventional radar systems through the reduction of the cost per sensor while maintaining a similar performance. This paper briefly discusses the use cases for such a sensor, the potential site locations considered, and a method for ranking site selection. The design of the sensor and its dedicated image processing chain is also discussed and, finally, the prototype implementation is described and the results from the test campaign using the prototype are presented and analyzed.

1. INTRODUCTION

With the Low-Cost Low-Earth Orbit Surveillance Sensor Array (LCLEOSEN) Deimos hopes to prove the capability to survey the full sky and process data in near real time. Radar systems are commonly used for this task due to their ability to work in more conditions than optical systems. However, radar systems are expensive to build and operate. LCLEOSEN is therefore designed to target a similar market by providing full sky coverage via an array of low-cost optical sensors.

With the aim of minimizing the overall system cost, the system is composed of Commercial Off-The-Shelf hardware components including a wide Field of View (FoV) lens, a high-sensitivity CMOS sensor and a dedicated image processing unit per telescope in the array, and a mount and dome for the array. Due to the large volume of data that can be gathered in a single night, the image processing unit is designed to operate in near real time to prevent a backlog of images. The telescopes are arranged in a grid pattern, with a slight overlap in the field of views to prevent coverage gaps, an example of a proposed configuration can be seen in Fig. 1.

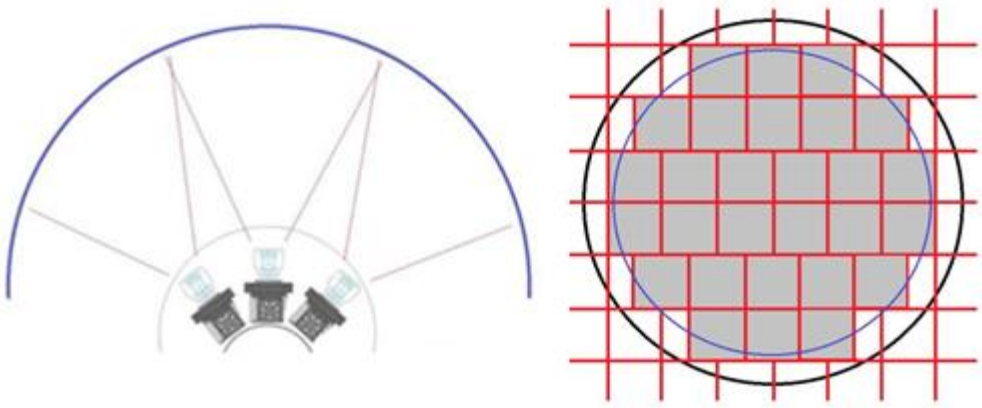

Fig. 1. LCLEOSEN Example Schematic

Each telescope has a low-cost Commercial Off-The-Shelf (COTS) lens of fixed focal length, and a sensor selected to match the area of the image projected from the lens, in order to minimize any unused area. The sensor selected also requires a reasonable resolution to allow it to detect Low Earth Orbit (LEO) objects. Finally, the image processing unit requires a high-performance processor and multiple CPUs to enable near-real time image processing.

Using the array of telescopes to enable full-sky coverage means that each telescope can be pointed in a fixed direction, thus a fixed mount can be considered. Due to the short exposure times used in this sensing application, sidereal compensation is not required, since the background stars apparent motion will be negligible. Finally, the array needs to be mounted inside a dome to protect it from the environment when not in use. A clam-shell type dome is the most appropriate choice to avoid interference with the telescopes view.

Besides the hardware the system also comprises of two main software modules: hardware control and image processing. The hardware control software needs to be custom built for each different hardware implementation, but can be adapted from similar existing systems, as was the case in this project; previous Deimos software was adapted for use with the new configuration.

The core of the work in this project was to build an automated image processing pipeline capable of detecting objects in captured images in near real time, while rejecting false artifacts, such as hot pixels or noise. There are two modes of extraction, one for point detections and one for trails. Whether an object appears as a point or trail is due to their difference in apparent angular speed, fast objects appear as trails, with decreasing length with decreasing speed to the extreme of a point detection. For a given exposure time: objects at zenith have the fastest apparent angular speed, decreasing with elevation, and objects in lower altitudes (with higher orbital velocities) have a higher apparent angular speed than those is higher altitude orbits. Varying the exposure time used allows an observer to vary the length of trails captured, however to keep Signal to Noise Ratio (SNR) high the trails should be kept relatively short. Keeping exposure time short can also allow multiple images of a space object to be captured before it escapes the FoV.

In order to accurately state that an object is detected in the images captured, a minimum of 3 single point detections (loners) of it are necessary, while in the case of trail a minimum of 2 aligned (i.e., the trails directions match) detections is sufficient. By increasing the minimum number of detections used as a threshold, it is possible to reduce the number of false detections or false positives (where an image artifact is falsely identified as an object). However, as the minimum number of detections increases, real objects with less detections could be falsely ruled out (false negative). The software developed in this project is designed to balance these factors to detect objects as efficiently but accurately as possible.

This paper builds on previous work, [1], and will discuss briefly the use cases and site selection method for the LCLEOSEN, then briefly cover the prototype implementation and observation campaign. The results of previous work are briefly recapped, then the additional data analysis is outlined, including the implementation of a new filter. The results of the extended analysis are presented and to wrap up the effect on the original project, conclusions are discussed and future work is outlined.

2. USE CASES

The primary use cases for a system such as LCLEOSEN stem from its capability to image the full sky, at any time (within given optical system limits; night time, no cloud cover, etc.). This full sky coverage allows tracking of objects without prior knowledge of their orbit and gives rise to many interesting use cases such as: gathering ephemeris on multiple targets simultaneously; discovery of new or lost objects; cross-cuing of narrow FoV sensors; maintaining custody of non-Keplerian objects; tracking re-entering objects; monitoring for companion objects or debris ejected from objects; and monitoring low-radar cross-section objects. This list is not exhaustive, but a summary of the key use cases. See Fig. 2 for the use cases in graphical form.

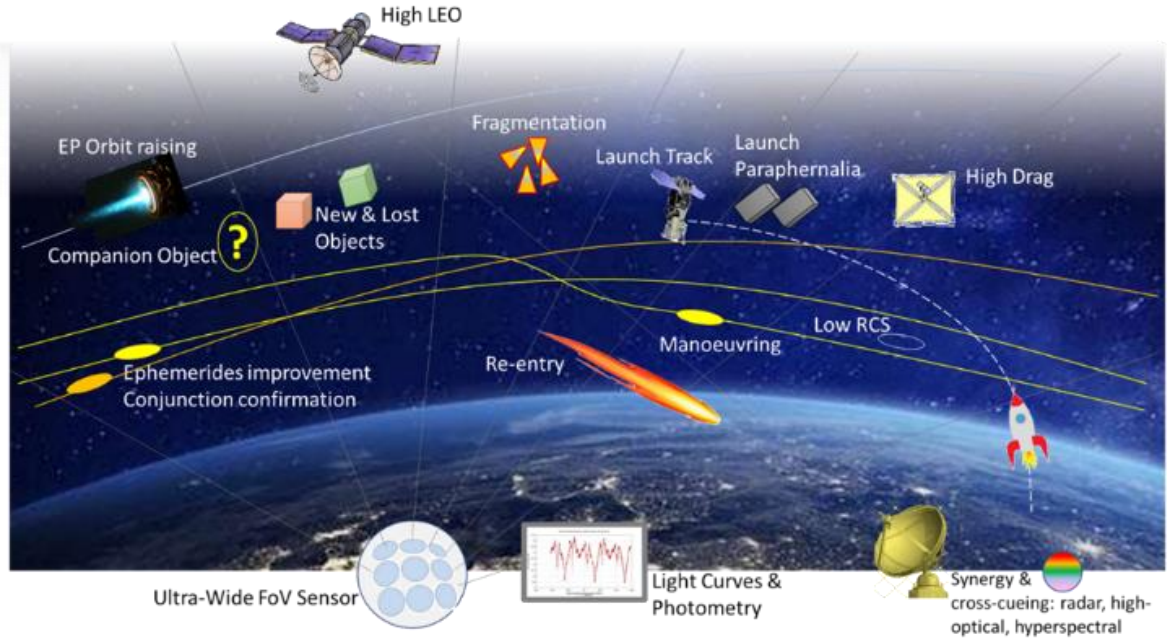

Fig. 2. Use Cases for LCLEOSEN

For a full discussion of the use cases please see previous work, [1].

3. SITE SELECTION

The selection of a site for a system such as this can be done in many ways, however, for this case a systematic scoring method has been developed based on practical metrics of a potential site. Three tiers of considerations have been developed. In Tier 1 the technical aspects affecting system performance are considered; such as Altitude, Latitude, Weather, etc. In Tier 2, logistical aspects are considered; including access to power and staff and ease of access to the site. Finally, in Tier 3, Optical interference sources are considered; such as air routes, aurora and other sources of optical interference. These considerations can be used to score each site and reduce a long list of possible sites to a short list of sites with good potential. See Fig. 3 for Tiers and considerations included.

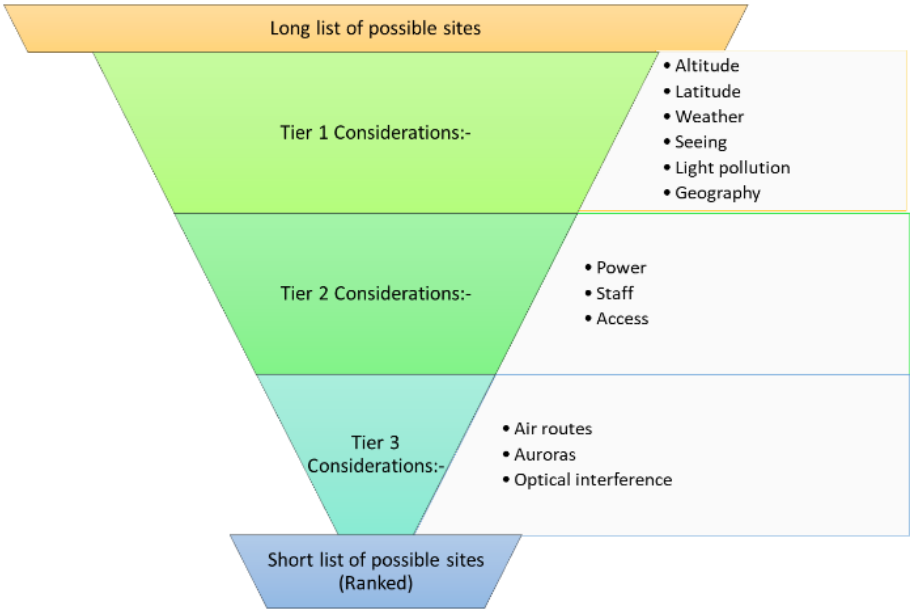

Fig. 3. Considerations for Down Selection of Potential Site

To score each consideration a scale of 1 to 5 is used, with 5 being the best. Where possible technical data is used in the scoring, for example: the Antoniadi Scale is used to score seeing, the Bortle scale is used to score light pollution, and to score the weather, the average number of cloud free nights a site gets is used. Once scores are assigned, the scores from each tier are weighted with a multiplier of 3 being applied to Tier 1 consideration, a multiplier of 2 applied to the Tier 2 considerations and 1 to the Tier 3 considerations. The multiplied scores are then totaled to give a single score for each site. The highest scoring sites being selected for the short list and the lowest scoring discarded. The short list can then be studied in greater detail to make a single selection.

4. PROTOTYPE IMPLEMENTATION

Over the course of January and February 2021, the prototype single telescope version of the LCLEOSEN system was implemented and tested briefly. Two lenses, an 85mm (25.4° FoV) and 105mm (20.8° FoV) lens were tested. The 105mm lens provided better angular resolution allowing detection of smaller objects. However, this comes at the cost of requiring additional telescopes in the final design to fulfill the full-sky coverage required. Since the prototype consists of a single telescope a simpler mount was required and the telescope could be sighted in an existing clamshell type dome at Deimos Sky Survey (DeSS) in Puertollano, Spain, see Fig. 4 and Fig. 5. For the sake of the prototype testing the system has been set to point to 0° azimuth and 61.5° elevation.

Fig. 4. Deimos Sky Survey clamshell domes

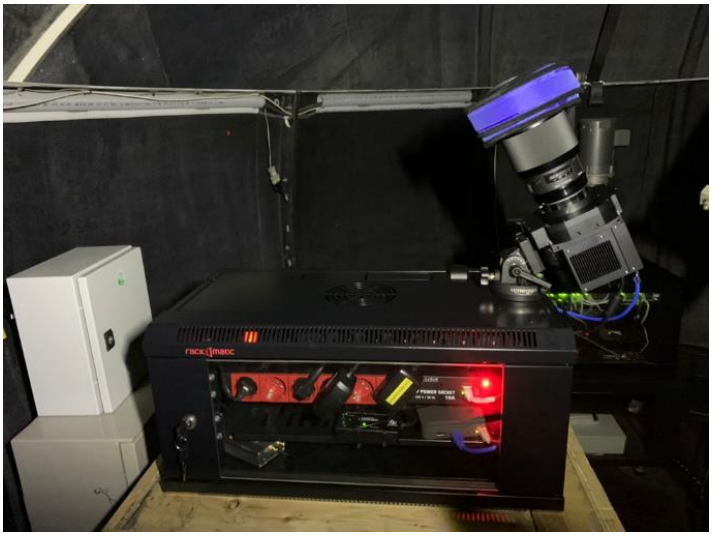

Fig. 5. LCLEOSEN prototype sensor mounted in DeSS dome

The black box shown in Fig. 5 contains the required subsystems; chronostamper, GOS antenna, controller and data exchange equipment. The data processing for the prototype has been done using a standard desktop computer with an 8-core Intel i9 processor with 3.6 GHz clock speed and 1 TB of SSD storage. The control computer was initially located in the control room, which resulted in a delay in the time between image captured, so it was relocated to the dome part way through the test campaign to reduce this delay. The first image was taken by the prototype (85mm lens) on January 24th 2021, see Fig. 6.

Fig. 6. First image taken with the LCLEOSEN prototype, fitted with the 85mm lens, on 24 January 2021

The software used to process images is divided into two parts; image processing and track detection. The first identifies elements in the image, and the second combines information from several images to identify an object track. More information on the software built is available in [1]. Since [1] was published the software has been updated, to remove some bugs, leading to different results herein.

5. OBSERVATION CAMPAIGN

Due to time restrictions on the project only 9 nights of observations were taken with the prototype during the test campaign. Previous work [1] showed the results of analysis of a small subset (4 partial nights, denoted by * in Table 1) of the campaign observations, here the data set analyzed has been expanded to include all 8 available nights. Note one night of data (16 Feb) has been omitted from both data set due to accidental data loss. The observations taken, including conditions taken under, are listed in Table 1.

Table 1. Test Campaign Summary

Data Set	1	2	3	4	5	6	7	8
Date	12 Feb	13 Feb	14 Feb*	15 Feb	17 Feb*	18 Feb*	22 Feb	23 Feb*
Lens	85 mm	85 mm	85 mm	85 mm	105 mm	105 mm	105 mm	85 mm
Image FoV	25.4°	25.4°	25.4°	25.4°	20.8°	20.8°	20.8°	25.4°
Pixel Scale	44.8 arcsec/pixel	44.8 arcsec/pixel	44.8 arcsec/pixel	44.8 arcsec/pixel	36.6 arcsec/pixel	36.6 arcsec/pixel	36.6 arcsec/pixel	44.8 arcsec/pixel
Exposure Time	0.1s	0.1s	0.1s	0.1s	0.2s	0.1s	0.1s	0.1s
Image Time Step	6-9s	6-9s	6-9s	6-9s	3s	3s	3s	3s
Observation Start Time	6.30 pm	6.30 pm	6.30 pm	6.30 pm	6.45 pm	6.45 pm	6.45 pm	6.45pm
Observation End Time	6.00 am	6.00 am	6.00 am	6.00 am	6.15 am	6.15 am	6.15 am	6.15 am
Number of Images Obtained	6808	7464	6904	7144	13544	13620	13112	14052

Note, as mentioned in Section 4, a change to the setup was made on 17 February. Before the 17th images were transmitted via internet connection for storage off-site, causing a delay between images, resulting in an image time step of 6-9s. Whereas after the 17th a hardline connection was established and the time step was reduced to just 3s. Since this change was made after the 85mm lens had been replace by the 105mm, it was decided to do one final night with the 85mm lens to compare the difference in the results that the timestep makes. One other test was made, testing the effect of the exposure time, on the 17th of February tests were conducted with a longer exposure time of 0.2s, whereas the rest of the nights were done with an exposure of 0.1s.

Due to the manual steps required in the testing (identifying false detections), the full data set has not been tested. Identifying false detections has to be done manually leading to a heavy manual labor burden, hence the first 1904 images captured each night are analyzed instead of the full set. The first images are selected as for LEO these occur at the times with most favorable lighting conditions, leading to large numbers of detections. The data set analyzed can be found in Table 2.

Table 2. Test Campaign Data Sample Selection

Data Set	1	2	3	4	5	6	7	8
Date	12 Feb	13 Feb	14 Feb	15 Feb	17 Feb	18 Feb	22 Feb	23 Feb
Lens	85 mm	85 mm	85 mm	85 mm	105 mm	105 mm	105 mm	85 mm
Observation Start Time	6.30 pm	6.30 pm	6.30 pm	6.30 pm	6.45 pm	6.45 pm	6.45 pm	6.45pm
Observation End Time	9.30 pm	9.30 pm	9.30 pm	9.30 pm	8.30 pm	8.30 pm	8.30 pm	8.30pm

Data Set	1	2	3	4	5	6	7	8
Total Time	3 h	3 h	3 h	3 h	1.75 h	1.75 h	1.75 h	1.75 h
Number of Images Selected	1904	1904	1904	1904	1904	1904	1904	1904

Previous work [1] discussed the non-linear relationships between processing power and processing time, and between the number of loners and the processing time. It also discussed the limits of magnitudes of real object detected in the data sets. Note, true limiting magnitude was not tested for, nor was the limiting size as a much more extensive campaign would be needed to support such a conclusion. However, an approximate magnitude limit of 9 was found for the 85mm lens and 10 for the 105mm. Above these magnitudes no real objects were detected.

The results discussed in the following sections discuss the further data analysis including the application of a new filter that assesses the elongation of loner trails to ensure its shape coherence between the multiple loners for each mover candidate. This filter does not affect the software performance, but does affect the false positive detection rate.

6. USE OF THE FILTER FOR THE 85MM LENS

In order to improve efficiency of the software at removing false detections a filter is proposed to ensure shape coherence between loners for a given mover. The results in Table 3 compare the results obtained for the 85mm lens when analyzing without and with the filter, and summarizes the differences in the result sets in terms of detection numbers and false detections.

Table 3. Results comparing the use of the filter for 85mm lens

		No Filter		Filter		Difference	
		N	%	N	%	Δ	Δ (%)
14 Feb	Total Detections	115	-	87	-	-28	-24.35
	Actual Detections	106	92.17	82	94.25	-24	-22.64
	False Positives	9	7.83	5	5.75	-4	-44.44
23 Feb	Total Detections	298	-	235	-	-63	-21.14
	Actual Detections	289	96.98	232	98.72	-57	-19.72
	False Positives	9	3.02	3	1.28	-6	-66.67

When comparing the detections for each night, it can be seen that the telescope performs much better on the night of the 23rd than on the 14th; this is due to the change in setup as discussed in Section 4, which reduced the timestep between images from 6-9s to around 3s. As a consequence, it is also easier for the software to separate real and false detections. The improvement in total detections is also partly due to the improvement in weather conditions on the night of the 23rd versus the 14th. From 12-15 February, the weather was partially cloudy which could have led to poorer seeing conditions on the night of the 14th.

It can be seen in the results in Table 3 that applying the filter has a significant impact on detection numbers, with a large reduction in total detections for both nights. However, it should be noted that in both cases it also results in an improvement in the number of false detections. The reduction in false detections, in percentage terms is good, however, when considering the full picture, it is recommended not to use this filter with the 85mm lens as it results in a much greater reduction in the number of true detections than false detections. For a similar actual detection rate

(92% without filter, 94% with the filter) many more detections are made without the filter, so it is judged to be too conservative for this telescope setup and is not recommended. It is suspected that the exposure time used is too short for many trails to be very elongated, and thus the filter comparing the shape isn't necessary.

The remaining three nights of data were processed without the filter applied, see Table 4. For these results again, it is hypothesized that the weather played a role, with increasing detections as the dates went on, corresponding to the improvement in weather conditions. However, without a check on the false negatives (the real objects missed by the sensor) it is impossible to confirm this hypothesis.

Table 4. Additional results for the 85mm lens

		No Filter	
		N	%
12 Feb	Total Detections	77	-
	Actual Detections	69	89.61
	False Positives	8	10.39
13 Feb	Total Detections	129	-
	Actual Detections	113	87.60
	False Positives	16	12.40
15 Feb	Total Detections	175	-
	Actual Detections	163	93.14
	False Positives	12	6.86

7. USE OF THE FILTER FOR THE 105MM LENS

For the 105mm lens, again the results with and without the filter applied are compared in Table 5.

Table 5. Results comparing the filter for the 105mm lens

		No Filter		Filter		Difference	
		N	%	N	%	Δ	Δ (%)
17 Feb	Total Detections	282	-	165	-	-117	-41.49
	Actual Detections	141	50.00	137	83.03	-4	-2.84
	False Positives	141	50.00	28	16.97	-113	-80.14
18 Feb	Total Detections	271	-	196	-	-75	-27.68
	Actual Detections	228	84.13	181	92.35	-47	-20.61
	False Positives	43	15.87	15	7.65	-28	-65.12

		No Filter		Filter		Difference	
		N	%	N	%	Δ	Δ (%)
22 Feb	Total Detections	239	-	191	-	-48	-20.08
	Actual Detections	235	98.33	188	98.43	-47	-20.00
	False Positives	4	1.67	3	1.57	-1	-25.00

The most notable result in Table 5 is the improvement in the false detection rate when using the filter for the night of 17th February. It should be noted that on the 17th, a longer exposure time was trialed, of 0.2s instead of 0.1s. With the longer exposure time, the elongation of trails is more pronounced and hence the filter works very well for this case. With the increase in noise and background stars captured due to the longer exposure time, more false loners appear in the images. However, the filter works well at distinguishing these and maintains a high number of the detections made without the filter. Hence the filter is highly recommended for the 105mm lens, with longer exposure times. This results also suggests that the filter could be recommendable for the 85mm lens when using a longer exposure time.

When considering the night with the shorter exposure time of 0.1s (nights of 18th and 22nd February), the use of the filter is not so easily decided. There is an overall reduction in the number of detections made for both nights, similar to that seen with the 85mm lens. However, there is a significant increase in false positives on the night of 18th February, and for this night the filter does well at reducing these false detections. However, the night of the 22nd shows no such improve due to the application of the filter, with very few false detections without the filter in the first place. It is suspected that the observing conditions played the largest role in the number of false positives on the night of the 18th February. Hence, it is difficult to conclude that the filter should or should not be applied but given the number of true detections missed, it is recommended that the filter not be applied, until further study can be completed.

One interesting anecdotal result, is that the filter seems to perform better when detections are close to the magnitude limits of the system. As such it could be applied only to those detections with a magnitude higher than a given threshold.

8. CONCLUSIONS AND FUTURE WORK

There are notable differences in the detection rates across the various nights of the campaign. Further analysis is recommended, before reaching final conclusions. However, it is concluded that the image processing filter proposed herein based on loner shape coherence should be applied when considering exposure times of 0.2s or longer. As an intermediate approach, the software could be run both with and without the filter, with only the additional detections made without the filter analyzed to confirm they are real. This would minimize the manual burden, while maximizing the real detections.

Previous work proposed the 85mm lens for the prototype full system, and while that conclusion still holds based on the results presented herein, the selection does not have to be final. Ideally, both lenses would be testing concurrently to show the differences in performance under the same conditions. However, the results herein show relatively equitable performance for both lenses, and as such it is recommended that the final system be customizable, with different lenses to meet a variety of needs.

In terms of future work, the major advance needed to confirm results and remove the manual checks is to implement an automatic correlation of a tracklet to a catalogue of objects. By implementing this automatic correlation, false negatives could also be tested. However, false positives identified by this means should still be checked manually in case they are real detections of objects not in the catalogue. This next step could be followed by a more intensive testing campaign to increase the data set available. Finally, a second prototype sensor could be used to compare the two different lenses under the same observing conditions.

9. ACKNOWLEDGMENTS

The original project this work builds on was done under a grant awarded by UKSA in the 'Advancing research into space surveillance and tracking' call.

10. REFERENCES

[1] E. Kerr,B. Del Campo Lopez, N. Maric, J. Nomen Torres, G. Falco, N. Sanchez Ortiz, C. Dorn, S. Eves. Design and Prototyping of a Low-Cost Leo Optical Surveillance Sensor. 8th European Conference on Space Debris, 2021.